

Article

Not peer-reviewed version

Optimized Wireless Sensor Network Architecture for AI-Based Wildfire Detection in Remote Areas

[Safiah Almarri](#)^{*}, [Hur Al Safwan](#), [Shahd Deya Al Qisoom](#), [Soufien Gdaim](#), [Abdelkrim Zitouni](#)

Posted Date: 21 May 2025

doi: 10.20944/preprints202505.1661.v1

Keywords: forest fire; hybrid WSN; energy efficiency; adaptive routing; artificial intelligence



Preprints.org is a free multidisciplinary platform providing preprint service that is dedicated to making early versions of research outputs permanently available and citable. Preprints posted at Preprints.org appear in Web of Science, Crossref, Google Scholar, Scilit, Europe PMC.

Copyright: This open access article is published under a Creative Commons CC BY 4.0 license, which permit the free download, distribution, and reuse, provided that the author and preprint are cited in any reuse.

Article

Optimized Wireless Sensor Network Architecture for AI-Based Wildfire Detection in Remote Areas

Safiah Almarri ^{1,*}, Hur Al Safwan ¹, Shahd Al Qisoom ¹, Soufien Gdaim ² and Abdelkrim Zitouni

¹

¹ Department of Physics, College of Science & Humanities Jubail, Imam Abdulrahman Bin Faisal University, Dammam, Jubail 31961, Saudi Arabia

² PRINCE Research Laboratory, ISITCom, Sousse University, Sousse 4011, Tunisia

* Correspondence: Safiamarri.2001@gmail.com; Tel.: +966556364621

Abstract: Wildfires are complex natural disasters that considerably impact ecosystems and human communities. Early detection and prediction of forest fire risk are necessary for effective forest management and resource protection. This paper proposes an innovative early detection system based on a Wireless Sensor Network (WSN) composed of interconnected Arduino nodes arranged in a hybrid circular/star topology. This configuration reduces the number of required nodes by 53–55% compared to conventional Mesh 2D topologies, while enhancing data collection efficiency. Each node is equipped with temperature and humidity sensor and uses ZigBee communication for real-time monitoring of wildfire risk conditions. This optimized topology ensures 41–81% lower latency and 50–60% fewer hops than conventional Mesh 2D topologies. The system also integrates artificial intelligence (AI) algorithms (multiclass logistic regression) to process sensor data and predict fire risk levels with 99.97% accuracy, enabling proactive fire mitigation. Simulation results for a 300 m radius area show the non-dense hybrid topology to be the most energy-efficient, outperforming dense and Mesh 2D topologies. Additionally, the dense topology achieves the lowest packet loss rate (PLR), reducing losses by up to 80.4% compared to Mesh 2D. Adaptive routing, dynamic round-robin arbitration, vertical tier jumps, and GSM connectivity ensure reliable communication in remote areas, providing a cost-effective solution for wildfire mitigation and broader environmental monitoring.

Keywords: forest fire; hybrid WSN; energy efficiency; adaptive routing; artificial intelligence

Introduction

Forests are vital for ecological balance, climate regulation, and resource provision, making their protection essential [1]. Although forest fires are a natural part of some ecosystems, they increasingly pose serious threats to both the environment and human life, especially under dry conditions, high temperatures, and strong winds [2].

Wireless sensor networks are a key technology for early forest fire detection, offering real-time monitoring with high accuracy and minimal human input [3]. By sensing parameters like temperature, humidity, and smoke, they enable timely responses that help prevent small fires from becoming large-scale disasters, reducing environmental, economic, and human risks [4].

WSNs, typically composed of thousands of low-cost, low-power smart nodes, can be deployed in various topologies such as star, tree, and mesh architectures [5–7]. They have significantly advanced wildfire detection and are widely applied in areas including environmental monitoring, target tracking, security, military defense, and healthcare [8, 9]. A key advantage of WSNs lies in their ability to integrate multiple energy sources, providing a stable and continuous power supply essential for sustained operation [10].

The sensor node is a core component of WSNs due to its critical role in establishing interconnectivity and enabling data acquisition. It is responsible for collecting, monitoring, and transmitting environmental data. Modern sensors are capable of measuring both dynamic and static

variables, such as humidity, land gradient, wind direction and speed, and smoke presence [11]. By utilizing sensor-based systems, it becomes possible to detect fires in their early stages and support informed decision-making for effective fire suppression.

ZigBee, based on the IEEE 802.15.4 standard, is commonly used in remote forest areas due to its low power consumption, reduced latency, and simplicity [12]. It supports communication over distances of 10 to 100 meters at a data rate of 250 Kbit/s, with extended range through mesh network topology [6]. This mesh topology is particularly beneficial for wildfire detection systems, allowing nodes to relay data through others, ensuring reliable communication even in dense forests [13].

To extend connectivity and integrate the local ZigBee sensor network with the internet, GSM technology is essential [14]. It enables communication between the sink node and the control center, offering broader coverage and internet access when available [15]. In wildfire detection systems, a central GSM node collects fire location data from sensor nodes and transmits it via SMS to the control center. With appropriate routing techniques, a single GSM node can connect to over 1,000 nodes, enabling comprehensive monitoring [16]. In areas without internet access, GSM ensures continuous data transmission via cellular networks, maintaining uninterrupted communication.

Artificial intelligence (AI) is increasingly used in wildfire detection systems to improve accuracy and response times. AI algorithms, including machine learning, analyze real-time sensor data to identify fire indicators such as temperature spikes and smoke, enabling faster detection and more efficient resource deployment [3].

The proposed fire detection system utilizes a hybrid star/circle topology, combining both centralized and mesh network configurations. This approach merges the energy-efficient data collection of the star topology with the robustness and redundancy of the mesh network, optimizing performance in dynamic wildfire environments. In wildfire-prone areas, this topology offers enhanced scalability, reliability, and efficiency. Additionally, the use of ZigBee for communication ensures reliable, low-power transmission while maintaining strong security protocols, essential for preserving data integrity in remote areas with high signal interference risks. To analyze real-time environmental data, the system employs artificial intelligence (AI) to enhance detection accuracy and predict fire behavior, thereby improving response effectiveness and wildfire management.

The remainder of the paper is organized as follows. We describe the related works in Section 2. We present the proposed architecture and methodology in Section 3. Effectiveness and efficiency evaluation results are described in Section 4. We conclude the paper in Section 5.

2. Literature Review

The detection of forest fires is a critical problem that has garnered significant attention in recent years due to its high environmental and economic impact, leading to the development of various technologies to overcome the limitations of traditional systems. WSNs are now central to modern wildfire detection, addressing the inefficiencies and delays of traditional methods such as towers, cameras, and satellites, which are limited by weather and image acquisition frequency [8].

Over the years, WSNs have evolved to address these challenges. Early studies focused on integrating WSNs with environmental sensors, including temperature, humidity, and smoke detection sensors, to create reliable, low-cost, and energy-efficient monitoring systems. In [17], Somov discussed the significant challenges in routing for energy efficiency in WSNs. Gomathi et al. presented a ZigBee-based system to enhance the reliability of fire detection while reducing delays and energy consumption. Sabit et al. emphasized the advantages of WSNs in real-time fire prediction, as their system provides superior spatial and temporal resolution compared to satellite-based approaches.

The integration of Artificial Intelligence (AI) and Internet of Things (IoT) has significantly enhanced wildfire detection systems by leveraging real-time environmental data and complex algorithms for more accurate and timely predictions. Bahrepour et al. pioneered AI-based fire detection systems, using AI to distinguish real from false alarms in residential fire systems. Ko et al. developed an intelligent WSN for early detection by analyzing real-time environmental parameters

like temperature and smoke. Recent advancements focus on combining machine learning (ML) and deep learning (DL) with WSNs for real-time wildfire prediction. For instance, Pradeep et al. proposed a robust ML framework leveraging AI for fire events in a variety of environments. Varela et al. applied information fusion techniques to enhance detection accuracy, achieving 100% detection in controlled settings and emphasizing energy efficiency for real-world applications. Recent works by Attia et al. and Bhamra et al. explored using machine learning to improve fire detection accuracy by analyzing sensor data for early prediction in diverse environments. These studies focus on dynamic WSN configurations and machine learning models to detect fire hazards early, even in remote areas [24, 25]. Yang et al. incorporated IoT-based WSN systems with advanced algorithms that fuse environmental data in real-time, optimizing power consumption and detection accuracy. In [27], Benzekri et al. incorporated deep learning to refine wildfire detection by identifying complex patterns in sensor data and images, making the system adaptable to diverse environmental conditions. In [28], Mahdianpari et al. developed a hybrid AI model combining CNN and RNNs to predict wildfires, significantly reducing false negatives in detection systems. AI models have been enhanced by hybrid IoT-AI systems combining real-time sensor data and satellite imagery. In [29], Avazov et al. integrated smoke and gas sensors with deep learning for fire classification, improving monitoring of large forest areas by reducing false alarms and enhancing detection accuracy.

The choice of network topology is crucial for optimizing WSN performance in wildfire detection systems. Various topologies, such as ring, star, mesh, and tree, have been explored, each with distinct benefits and limitations. Mulligan et al. highlighted the importance of coverage in WSNs and the trade-offs between different deployment schemes. Abbasi et al. reviewed energy-efficient topology control techniques to enhance data transmission and network efficiency in wireless ad-hoc networks. To address the limitations of traditional WSN configurations, some studies have proposed hybrid and dynamic topologies. For instance, Jiang et al. introduced a hybrid topology that merges star and mesh structures to enhance coverage and fault tolerance in wildfire-prone areas, optimizing energy use and communication efficiency for reliable fire detection and fast data transmission.

In WSNs for wildfire detection, efficient energy use is vital due to remote deployment locations. Recent research has focused on techniques like duty cycling, adaptive transmission power control (ATPC), and renewable energy harvesting. Cheour et al. advanced this area by integrating hybrid solar and wind energy into a WSN model, significantly extending sensor node lifespan in remote forest areas where long-term deployment is essential.

3. WSN Architecture

The proposed star/circle WSN topology seeks to create a sustainable, efficient monitoring system for long-term sensor node deployment across diverse forest types. A key aspect of the methodology is determining the optimal number and arrangement of sensors for balanced coverage. Strategic deployment tackles challenges posed by varying forest conditions, while efficient placement is essential for testing routing protocols, optimizing connectivity and data integrity over different distances and densities, and overcoming communication barriers in dense canopies.

3.1. Star/Circle Topology

In the proposed WSN topology, nodes are arranged in concentric flat or pyramidal circles based on forest type (flat or mountainous), as illustrated in Figure 1. The network design considers forest density, terrain, and the use of Zigbee protocol for node communication. Operating at 2.4 GHz, Zigbee may face interference from other wireless signals (e.g., Wi-Fi, Bluetooth), especially near urban areas. However, this is negligible in the targeted remote forests. Terrain features like hills, as well as weather conditions such as rain or fog, can further reduce signal range. Under optimal conditions, Zigbee can reach 50 - 100 meters, but in dense vegetation, the range may drop to 10–20 meters or less. These factors are accounted for in the WSN architecture and sensor node deployment.

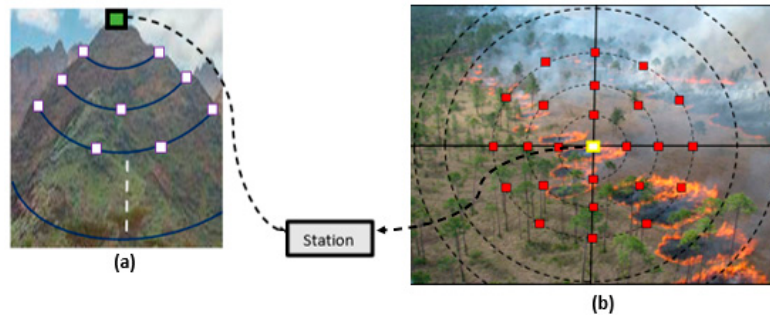


Figure 1. Deployment of WSN nodes in: (a) mountainous and (b) flat forest scenarios.

The WSN architecture (Figure 2) combines two topologies: star and circle. In star topology, a central sink node is surrounded by four sensing nodes aligned along its axes. Due to the distance exceeding their sensing range, these nodes cannot communicate directly with each other. Instead, they transmit data to the sink node upon detecting fire or act as intermediaries to relay data from nodes in the surrounding circular tiers.

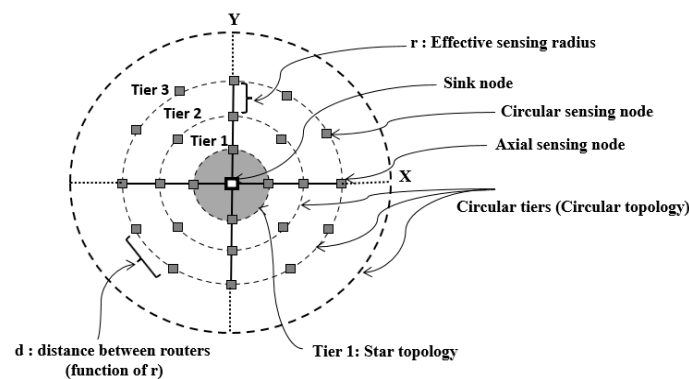


Figure 2. The proposed WSN architecture.

The circular tiers are centered around the sink node, with radii increasing by multiples of $n \times r$, where r is the effective sensing radius. Key nodes are placed along the axes at angles 0 , $\pi/2$, π , and $3\pi/2$ in each tier. The spacing between consecutive axis nodes equals the effective sensing radius, determined by forest type, density, and terrain. Within each tier, adjacent nodes are placed at distances less than or equal to r , ensuring reliable communication when needed.

In non-dense forests, the distance between circular tiers may exceed the effective sensing radius. In this case, data is relayed between nodes along the same circle until it reaches an axis node, which then forwards it to the sink. In dense forests, tier spacing is reduced to within the maximum effective radius, enabling communication between adjacent tiers. This allows faster data transmission during fire spread, enhancing responsiveness.

3.2. Nodes Deployments

A key challenge in WSN architecture design is balancing energy efficiency with full area coverage, which requires optimal sensor density. As the distance from the network center increases, circle radius grows, necessitating more nodes per tier. Based on node count and spacing, a network may be classified as dense or sparse. The proposed deployment strategy features low density (compared to typical mesh networks), flexibility, and adaptability to different forest types and terrains. It also ensures a balanced and organized layout.

To calculate the total number of sensing nodes: each circle includes 4 mandatory axis nodes. The number of nodes in one-quarter of a circle (between two axis points) is computed first, then multiplied by four to get the total per circle. These nodes are evenly spaced between axes, based on

their number, the circle's radius, and the effective sensing radius. The overall node count includes all circular tier nodes plus the 4 star-tier axis nodes. Consider that:

- N: total number of sensing nodes in the network,
- A: area of the forest,
- R: radius of the flat forest area,
- N_c: total number of circular tiers,
- r: effective sensing radius,
- d: distance between two neighboring nodes on a circle (dependent on r),
- N_i: index (order) of the circle,
- n: number of nodes in a circle.

The area of a flat forest is given by: $A = \pi R^2$. Therefore, the radius of the forest area is:

$$R = \sqrt{\frac{A}{\pi}}. \text{ The total number of circles is then: } N_c = \frac{R}{r} = \sqrt{\frac{A}{\pi r^2}}.$$

Equation (1) gives the total number of sensing nodes in the WSN:

$$N = 4 + \underbrace{4\{\lfloor 2r\pi/4r \rfloor + 1\}}_{\text{Number of nodes between two axes of the second circle}} + \underbrace{4\{\lfloor 3\pi r/4r \rfloor + 1\} \dots 4\{\lfloor N_c r\pi/4r \rfloor + 1\}}_{\text{Number of nodes of the circle order } N_c} \quad (1)$$

Number of star nodes Number of nodes of the second circle Number of nodes of the circle order N_c

Note that the function $\lfloor x \rfloor$ represents the floor function to ensure integer node counts. For example, $\lfloor \frac{2\pi}{4} \rfloor = 1$. The simplified network density equation (Equation (1)) is given by the Equation (2).

$$N = 4N_c + 4 \sum_{i=1}^{N_c} \left(\left\lfloor \frac{i\pi}{4} \right\rfloor + 1 \right) \quad (2)$$

Once the number of nodes is determined, the next step is to calculate the spacing distance, d , between each pair of nodes. To compute the spacing between nodes in each quarter of a circle with order N_i , the corresponding circle radius R_i is calculated as a function of the effective sensing radius r ($R_i = N_i r$). Multiplying this radius by the quarter angle $\frac{\pi}{4}$ gives the total distance between the two axis nodes of the circle, i.e., $N_i r \times \frac{\pi}{4}$. Assuming n is the number of nodes required in a quarter of the circle ($n = \lfloor \frac{N_i \pi}{4} \rfloor$), the total distance is divided by $(n + 1)$. Thus, for any circle of order N_i , the distance d between nodes is given by Equation (3):

$$d = \frac{N_i \pi}{4} \times \frac{r}{n+1}; n = \lfloor x \rfloor = \left\lfloor \frac{N_i \pi}{4} \right\rfloor \Rightarrow d = \frac{N_i \pi r}{4(\lfloor \frac{N_i \pi}{4} \rfloor + 1)} \quad (3)$$

For example, in a forest area with $R = 1000$ m and an effective sensing radius $r = 100$ m (topology with one star and 9 circles), the spacing distance d for $x = \frac{6\pi}{4} = 4.71$ ($n = \lfloor x \rfloor = 4$), is calculated as: $\frac{6\pi}{4} \times \frac{r}{5} = 94.2$ m.

3.3. Routing Algorithms and Applications

Forests vary greatly in density and topography, ranging from dense, tall-tree areas to open, sparsely vegetated spaces, with terrain that can be flat or mountainous. This diversity requires a highly adaptable and flexible WSN for effective environmental monitoring. To address these challenges, a hybrid network system combining multiple structures will provide comprehensive coverage and efficient data transmission across different forest conditions. The hybrid WSN architecture ensures adaptability in both dense and open terrains, whether flat or rugged. This flexibility allows for the optimization of sensor numbers, efficient deployment, and the selection of appropriate routing algorithms. Different routing algorithms can be employed in the proposed network configurations. Mixed forests where some areas are treeless, and others are dense or sparse can be also encountered. In these forest types, the WSN design excludes the treeless regions, focusing

on the other region to deploy the sensing nodes. Figure 3 illustrates some examples of truncated flats and mountainous forests and the corresponding nodes deployments.



Figure 3. Examples of mixed forests: (a) truncated flat forest, and (b) truncated mountainous forest.

The proposed WSN architecture supports the integration of adaptive, semi-adaptive, and deterministic routing algorithms, tailored for wildfire detection. Adaptive routing dynamically adjusts paths to network changes, ensuring rapid rerouting during failures—ideal for dense forests requiring emergency responsiveness. Semi-adaptive routing balances flexibility and cost, using fixed paths but adapting selectively, reducing overhead for non-critical tasks. Deterministic routing is limited to redundant setups. For non-dense forests, a hybrid adaptive-semi-adaptive approach optimizes adaptability and efficiency. A dynamic arbitration scheme resolves conflicts by prioritizing critical data (e.g., fire alerts), queuing lower-priority transmissions to prevent deadlocks and ensure timely delivery to the central host. Dynamic arbitration is used to ensure equitable data processing, preventing any node from being indefinitely delayed. This hierarchy ensures robustness across varying forest topologies and operational demands.

3.3.1. Routing in Dense Forests

In dense forests, network tiers are positioned closely (inter-tier distance \leq effective sensing radius) to address high environmental obstruction density. This proximity enables adaptive routing algorithms to dynamically reroute data around obstacles (e.g., thick vegetation) through adjacent upper/lower tiers if intra-tier paths are blocked. Critical alerts (e.g., wildfires) bypass blockages via these verticals reroutes, ensuring delivery to the control center. Inter-tier communication enhances resilience by allowing direct data jumps between tiers, eliminating dependency on horizontal paths. In mountainous terrain, nodes adopt a conical configuration around peaks to maximize coverage across elevations while maintaining tiered connectivity. Figure 4 illustrates an example of possible inter-tier adaptive routing in the case of a flat forest.

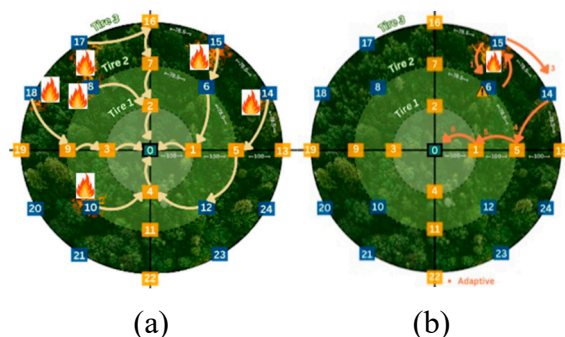


Figure 4. (a) Example of inter-tier routing in flat forest, (b) failed node scenario.

In this example, fires are detected at nodes 8, 10, 14, 15, 17, and 18. The adaptive routing algorithm aims to minimize energy use and avoid unnecessary transmissions. Figure 4.a illustrates possible paths for forwarding fire alerts to the sink node. For instance, node 14 sends data to node 5 in the lower tier. When node 5 detects that axis node 1 is busy handling data from node 15 via node

6, it forwards the message to node 12. To reduce latency and prevent data blocking, node 12 routes through node 4, which may also be receiving from node 10. If nodes 10 and 12 simultaneously request access to node 4, dynamic arbitration decides the priority - e.g., if node 12 arrives first, node 10 is queued. Alternatively, node 5 could wait until axis node 1 becomes free. Adaptive inter-tier routing also proves effective when nodes fail. As shown in Figure 4.b, if node 15 detects that node 6 is inactive, it reroutes its data through node 14 to maintain communication continuity.

3.3.2. Routing in Non-Dense Forests

In non-dense mountainous and flat forests, where vegetation and trees are sparsely distributed, the number of WSN tiers and nodes is optimized accordingly. The spacing between consecutive circles can exceed the maximum sensing radius, concentrating nodes in areas with vegetation. Axis nodes are always present, with consecutive ones separated by the effective sensing radius. In this setup, inter-tier routing is disabled - nodes cannot transmit across different tiers. The hybrid Adaptive-Semi-Adaptive routing algorithm is ideal here. Nodes within each tier are divided into quadrants, and data transmission is limited to neighboring nodes within the same tier and quadrant, either clockwise or counterclockwise. Data is relayed within the circle until it reaches the appropriate axis node, which then forwards it along the axis path to the sink node.

Figure 5 illustrates the application of the hybrid Adaptive-Semi-Adaptive routing in forest fire scenarios. Inter-tier and inter-quadrant communication is restricted, allowing only clockwise and counterclockwise data flow within the same quadrant and tier. Fires are detected at nodes (0, 4, 6, 8, 9, 14, 15, 18, 20). Blue arrows represent data originating from the node itself, while red arrows indicate forwarded data. Nodes 1 to 4 on the star-shaped circle send data directly to the sink. Node 15 routes its data to the nearest axis node 16, which forwards it along the axis to the sink. If node 7 receives simultaneous data from node 6, a two-level dynamic arbitration is applied. Similarly, node 9, which has a fire and receives data from nodes 8 and 19, triggers a two-level arbitration if data arrives at once. In case of a fire at the sink (node 0) while receiving data from its four surrounding nodes, a five-level dynamic arbitration ensures GSM-based transmission to the control center proceeds smoothly.

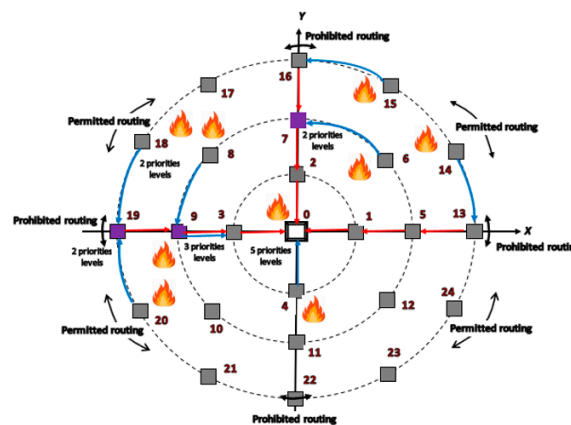


Figure 5. Example of hybrid Adaptive-Semi-Adaptive routing for fire traffic.

3.4. Latency and Packet Loss

The total end-to-end latency L is calculated using the following Equation (4) [34, 35].

$$L = h \cdot (t_{tx} + t_{proc} + t_{queue}) + t_{reroute} \quad (4)$$

With: h : number of hops, t_{tx} : transmission time per hop, t_{proc} : processing time per node, t_{queue} : queuing delay per node, $t_{reroute}$: additional delay due to adaptive rerouting.

For the hybrid dense topology, the vertical rerouting enables direct jumps between tiers (concentric circles), eliminating intra-tier detours. Each tier has a **radius increment of 100 meters** (distance from the sink). Therefore, the **diameter increment per tier** is $2 \times 100 \text{ m} = 200 \text{ m}$. The number of hops is given by Equation (5).

$$h = \sqrt{\frac{\text{Diameter}}{\text{Tier diameter increment}}} = \sqrt{\frac{\text{Diameter}}{200}} \quad (5)$$

In fact, since hybrid dense topology allows data to jump vertically between tiers, bypassing horizontal obstacles, the number of hops is reduced compared to purely horizontal routing. The square root reflects the multi-dimensional optimization of the network.

For the hybrid non-dense topology, there is no vertical rerouting, and data travels intra-tier to axis nodes, then sequentially to the sink. The number of hops is given by Equation (6).

$$h = \frac{\text{Diameter}}{200} + \log_2\left(\frac{\text{Diameter}}{200}\right) \quad (6)$$

In fact, in non-dense topology, vertical rerouting between tiers is disabled. Instead, data must travel **horizontally within the same tier** until it reaches an **axis node**. This introduces two components to the total hop count (**Tier-to-Tier Hops**: Basic linear scaling with diameter ($\frac{\text{Diameter}}{200}$), and **Intra-Tier Detours**). **Intra-Tier detours** are additional hops required to navigate within a tier to reach the nearest axis node. The logarithmic term approximates the average number of **detour hops** needed to reach an axis node within a tier as the network scales. It ensures the hybrid topology remains efficient in non-dense forests, even without vertical rerouting. This approach balances realism and simplicity, reflecting observed routing behavior in sparse deployments.

The above equations show that the proposed topology requires fewer hops than the 2D Mesh, which suffers from linear hop growth and no vertical rerouting, causing higher latency. The number of hops in the case of the 2D Mesh topology is given by Equation (7).

$$h = \frac{\text{Diameter}}{\text{Average hop distance diameter}} = \frac{\text{Diameter}}{50} \quad (7)$$

In fact, the 2D Mesh topology, nodes are placed in a grid where each node communicates directly with its immediate neighbors (up, down, left, right). So, the **average hop distance** (50 m) ensures reliable communication between nodes while balancing signal strength.

The Packet Loss Rate (PLR) depends on the topology number of hops h as shown in Equation (8) [36, 37]. So, packet PLR varies significantly across the proposed topology and the 2D Mesh topology due to differences in routing efficiency and hop-count scaling.

$$PRL = 1 - \prod_{l=1}^h (1 - P_{loss,i}) \quad (8)$$

3.5. Sensor Nodes Arbitration

ZigBee, based on IEEE 802.15.4, is optimized for low-power, low-data-rate wireless communication [38]. Efficient packet structure is essential for performance. In the proposed design (Table 1), the payload allocates two bytes for device ID, two for a unique header (UH) to ensure reliable delivery, one byte for priority and status flags (e.g., battery level, sensor errors), and two bytes for temperature and humidity readings.

Table 1. Payload frame.

UH	ID	Priority level	Temperature	Humidity
2 bytes	2 bytes	1 byte	1 byte	1 byte

Unlike static arbiters, dynamic arbiters can adjust priority orders in real time [39], enabling more effective bandwidth allocation. Their primary advantage lies in their ability to prevent starvation, making them well-suited for shared-access systems such as Multiprocessor Systems on Chip (MPSoC) and Networks on Chip (NoC), especially in asynchronous systems [40 – 44]. In WSNs, arbitration schemes address issues of fairness and starvation while optimizing energy consumption during communication [45 – 49]. These schemes are typically implemented on the Medium Access Control (MAC) layer, where conventional protocols often lack prioritized channel access and may suffer from inconsistent fairness.

To handle access conflicts in the proposed forest fire detection system, where multiple sensor nodes may simultaneously attempt to reach the same intermediate node, a dynamic arbitration mechanism is implemented within each router. This mechanism assigns priorities based on fire urgency, reducing the average response time to the control center. Each data frame includes two priority bits (high: 10, medium: 01, low: 00) embedded as the first two bits of the priority level byte. Priority is determined by fire severity and the estimated likelihood of occurrence, as evaluated by an AI model analyzing temperature and humidity data.

Under the proposed strategy, the sensor node with the highest priority is granted access during each request. If multiple nodes share the same priority, access is rotated in a round-robin manner after each successful transmission. Once access is granted, the requesting node is moved to the end of the priority queue, preventing resource domination and ensuring fair access. Figure 6 illustrates the round-robin priority shift: when requester X_i seeks access and X_j was the most recently served, X_j holds the lowest priority. X_i gains the highest priority only if none of the requesters between X_{j+1} and X_{i-1} have submitted access requests.

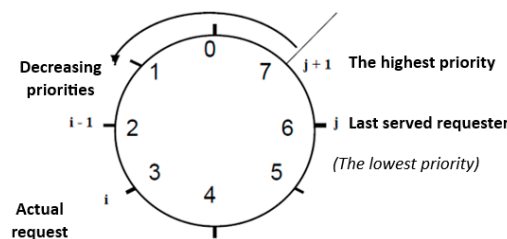


Figure 6. Round-robin priorities shift mechanism.

Based on the above specifications, the round-robin algorithm implemented in the sensor node arbiter is illustrated in Figure 7.

```

Wait until any  $X(i) = 1$  for  $i = 0$  to  $n-1$ ;
status =  $X(0 : n-1)$ ; // Array indicating active requests
Nb = CalculateRequesterNumber(status); // Determine number of active requests
switch (Nb) {
  case 1:
     $i = N(\text{status})$ ; // N is the rank register
     $Z(i) = 1$ ; // Grant access to the highest priority requester
    Wait until  $X(i) = 0$ ; // Wait until the requester finishes access
     $Z(i) = 0$ ; // Deactivate the grant
     $j = \text{FetchPriorityOrder}(P, i)$ ; // Determine the order of the granted requester
     $P = \text{Concatenate}(P[j + 1] \text{ to } n-1, P[0 \text{ to } (j - 1)], P(j))$ ; // Update priority list in round-robin manner
  .
  .

```

Figure 7. Round-robin algorithm.

3.6. AI-Based Fire Risk Prediction Approach

To enhance fire hazard prediction and improve system accuracy, artificial intelligence (AI) techniques were integrated into wireless sensor network (WSN) nodes. For predictive modeling, Multiclass Logistic Regression algorithms were used to derive equations that relate temperature and humidity measurements to the three fire risk levels: low, medium, and high [50]. These models were

trained on real environmental data, enabling the system to adapt to various conditions. Once the data packet is received and verified, the receiver computes the fire risk probability using Equation (9):

$$f = at + bh + c \tag{9}$$

Here, t is temperature, h is humidity, a and b are coefficients from training that reflect their influence, and c is a bias term to improve accuracy. This equation was developed through several stages. Initially, a large meteorological dataset containing temperature, humidity, and other weather variables (wind speed, pressure, visibility) from 13 cities in Saudi Arabia was used, including over 249,000 recorded entries [51].

The digitized data was divided into training and testing sets to ensure effective evaluation. Temperature and humidity served as inputs, while fire risk levels were the outputs. To handle classification, a multi-class logistic regression model was built using the scikit-learn library. It was configured to classify inputs into the three risk categories. During training, the model adjusted coefficients (a , b) and the bias term c to link inputs with risk levels. It produced three output values (f_1 , f_2 , f_3), each representing a fire risk category. The highest value determined the final risk classification.

4.Experimental Results

The performance of the proposed system was evaluated using Proteus 8 Professional and CapCarbone simulation tools [52, 53].

4.1. Proteus Simulation

Proteus was used to simulate the hardware functionality of both the transmission and receiving nodes. Each node was built around an Arduino Uno microcontroller. The transmission node incorporated a DHT11 sensor to measure temperature and humidity and used an XBee ZigBee module for wireless communication. The receiving node, also equipped with an XBee module, relayed the data to a central monitoring station via a GSM SIM900D module. This module sends alert notifications over the mobile network, including the fire status, its computed index, and the corresponding temperature and humidity readings [55].

Multiclass logistic regression is used for predictive AI modeling to classify fire risk based on temperature and humidity. The categorical fire risk variable is encoded numerically (0 = Low, 1 = Medium, 2 = High) to enable supervised learning. The model is trained using an 80/20 train-test split and achieves 99.97% accuracy, evaluated with a custom accuracy function. Decision boundaries are visualized to illustrate how the model distinguishes between risk levels. The system also supports real-time prediction for new inputs and calculates raw scores using the model’s learned coefficients.

Figure 8.a illustrates the relationship between temperature (x-axis), humidity (y-axis), and fire occurrence (color scale). Each point represents a data sample, with color intensity reflecting fire likelihood on a continuous scale from 0 (no fire) to 2 (high risk). The plot shows that high temperatures and low humidity correlate with increased fire risk, highlighted by the concentration of yellow points in the lower-right region.

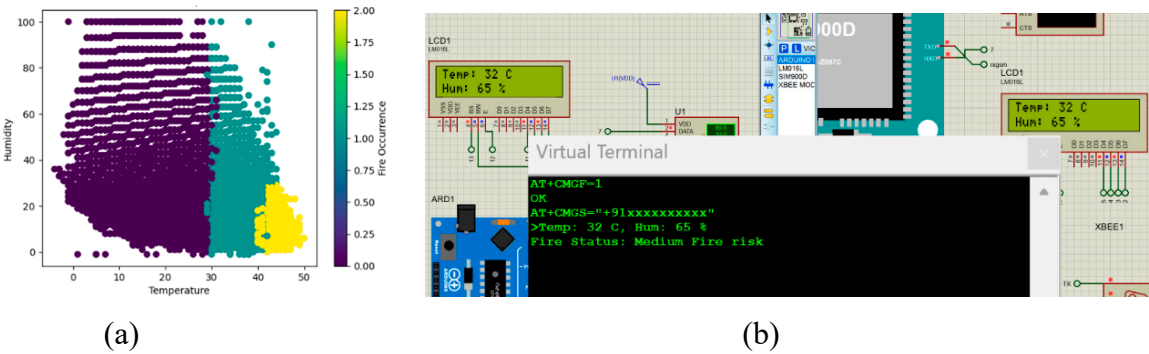


Figure 8. (a) Correlation between temperature, humidity, and fire occurrence, and (b) Fire risk output values for input conditions: Temperature = 32°C, Humidity = 65%.

As illustrated in Figure 8.b, for a temperature of 32°C and a humidity level of 65%, the three output values (Equation (10), (11), and (12)) generated by the equation corresponding to the fire risk levels are as follows:

$$f_1 = -10.75t + 0.084h + 350.05 \approx 11.45 \quad (10)$$

$$f_2 = 1.13t + 0.07h - 0.22 \approx 40.50 \quad (11)$$

$$f_3 = 9.62t - 0.15h - 349.83 \approx -51.95 \quad (12)$$

Since the highest value corresponds to equation f_2 , the resulting risk level is classified as medium, which aligns with the simulation result as shown in figure.

4.2. WSN Simulation

The CapCarbon Network Simulator was used to evaluate the topology, routing, and energy efficiency of the wireless sensor network (WSN) across different forest environments. Simulations covered both dense and sparse forest scenarios, with performance compared to the conventional 2D Mesh topology. Three routing techniques were implemented: Adaptive Inter-tier Routing (for dense forests), Hybrid Adaptive-Semi-Adaptive (for sparse forests), and Adaptive Routing for the 2D Mesh. Figure 9 shows two WSNs designed with CupCarbon for Mesh 2D and Star/Circle topologies.

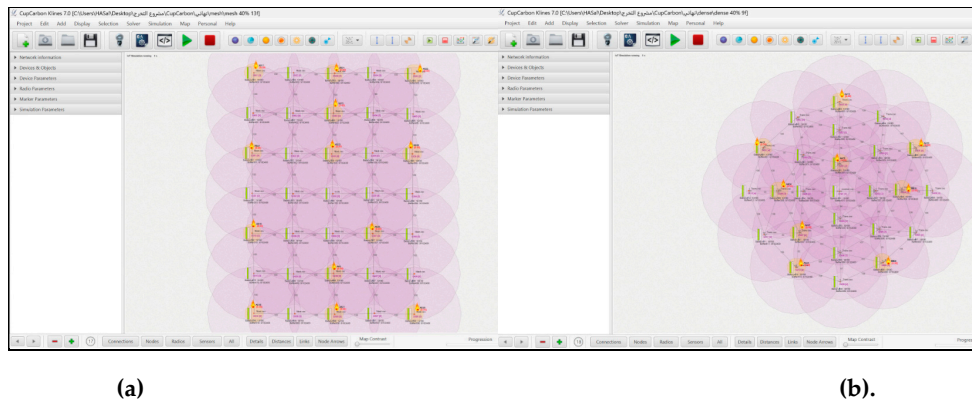


Figure 9. WSN Topologies designs using CupCarbon, (a) Mesh 2D, and (b) Star/Circle.

4.2.1. Topology Deployment Efficiency

The proposed Star/Circle topology employs structured circular arrangements to prioritize coverage in high-risk wildfire zones while reducing redundant node deployment. Figure 10 presents a comparison of node distribution strategies in WSN-based wildfire detection, contrasting the conventional 2D Mesh topology with the proposed Star/Circle approach. The node count for the 2D Mesh topology is calculated using Equation (13) [56].

$$N = \frac{2A\pi}{r^2\sqrt{27}} \quad (13)$$

The results show that as the monitored area increases, the Star/Circle topology becomes significantly more efficient than the 2D Mesh. While both topologies require the same number of nodes at small scales (e.g., 100 m radius), the Star/Circle approach reduces node count by 53% at a 1,500 m radius and by 55% at 3,000 m. This highlights its advantage in large-scale wildfire detection by improving energy efficiency and lowering deployment costs.

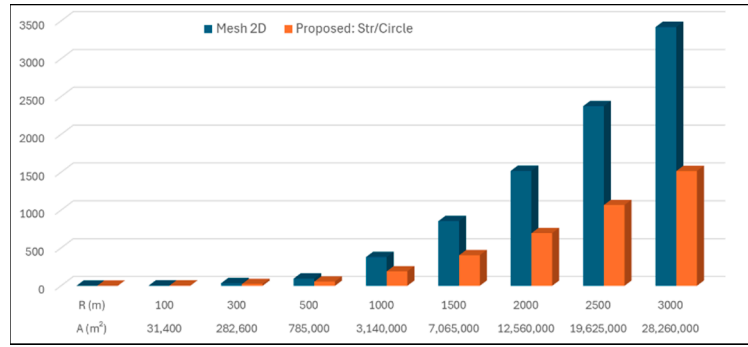


Figure 10. Comparison of Star/Circle and 2D Mesh Topology Deployments.

4.2.2. Latency and Packet Loss Analysis

Figure 10 presents tests conducted for forest areas with diameters ranging from 500 m to 3,500 m. The total end-to-end latency L is calculated using Equation (4), assuming identical operating conditions across the three topologies. ($t_{tx} = 0.2$ s, $t_{proc} = 0.1$ s, and $t_{queue} = 0.3$ s, $t_{reroute} = 0.5$ s).

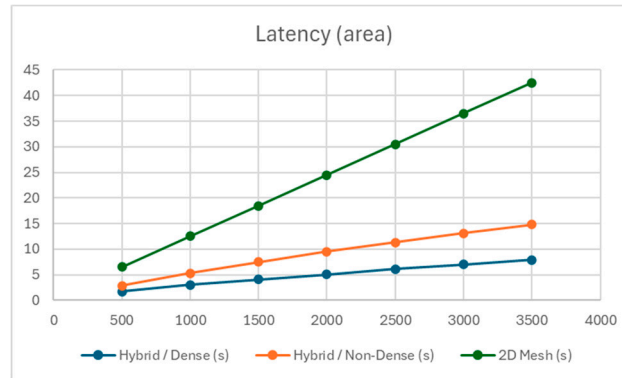


Figure 11. Latency comparison between star/circle and 2D Mesh topologies.

The test results indicate that the proposed hybrid star/circle topologies demonstrate a significant latency advantage over the traditional 2D Mesh topology. The hybrid dense topology leverages vertical rerouting between tiers (with 100 m radius increments), reducing hop counts by 50–60% compared to non-dense and 2D Mesh topologies. This structural efficiency enables the dense hybrid architecture to achieve 41–47% lower latency than the non-dense hybrid and 73–81% lower latency than the 2D Mesh. The non-dense hybrid, while constrained by intra-tier routing, still outperforms the mesh by 55–65% due to axis-based path optimization. While the non-dense hybrid lags slightly behind its dense counterpart, both significantly outperform the mesh in terms of energy efficiency and resilience to obstacles.

The Packet Loss Rate is calculated using Equation (14). Despite assuming a uniform per-hop loss, the proposed Star/Circle topology outperforms the 2D Mesh in terms of packet delivery efficiency ($P_{loss,i} = 0.02$) as shown in Figure 12.a.

$$PRL = 1 - (1 - 0.02)^h = (1 - 0.98)^h \quad (14)$$

PLR varies significantly across the three network architectures due to differences in routing efficiency and hop-count scaling. The dense hybrid Star/Circle performs best, with PLR rising gradually from 3.96% (500m) to 14.87% (3500m). The non-dense hybrid shows faster PLR growth, reaching 31.09%, while the 2D Mesh performs worst, with PLR climbing to 75.81% due to inefficient scaling. At 3500m, the dense hybrid reduces PLR by 52.2% compared to the non-dense hybrid and by 80.4% compared to the 2D Mesh. These results highlight the importance of efficient, adaptive inter-tiers routing. Dense hybrid's design limits hop buildup, making it ideal for real-time, low-latency applications like wildfire detection.

Figure 12b presents the simulation results generated by the CapCarbone tool for a 300 m area, considering that ZigBee/IEEE 802.15.4 is limited in range and sensitive to interference, and that sleeps are not scheduled. These results show that the dense hybrid Star/Circle topology achieves the lowest PLR for all fire diffusion percentages (20%–80%), with a 17.3% improvement over 2D Mesh and 11.7% over non-dense at 60% diffusion. At 80%, dense maintains 80.2% PLR, while non-dense and Mesh 2D exceed 91%. These high PLR values are explained by the fact that non-dense and Mesh 2D topologies are more affected by simulation considerations about ZigBee limitations and the absence of sleep scheduling. As fire spreads, node failures increase, degrading connectivity and amplifying packet loss. This explains that the dense topology’s adaptive routing dynamically reroutes data around compromised nodes, whereas non-dense and Mesh 2D networks suffer from redundant hops and inflexible paths.

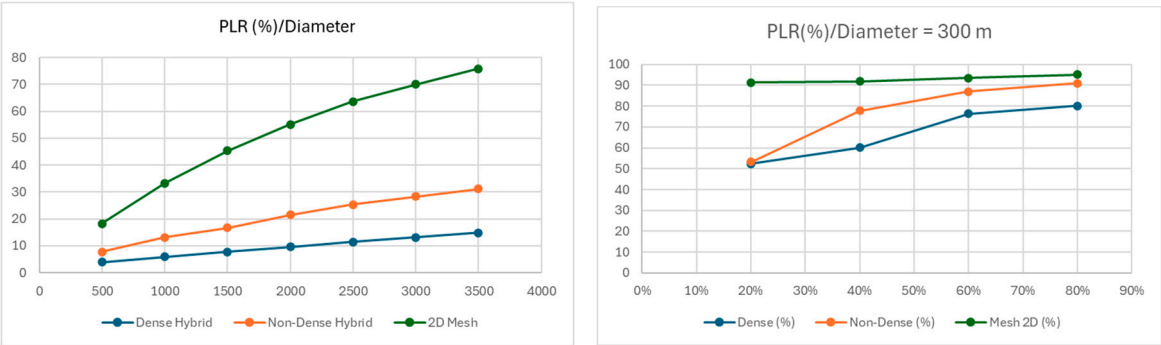


Figure 12. PLR Comparison Across Topologies: (a) Varying Diameters, (b) Diameter = 300 m.

4.2.3. Energy Dissipation Analysis

The simulation results generated by the CapCarbone tool (Figure 13) for a 300 m area demonstrate distinct energy dissipation patterns across the three network topologies, dense, non-dense, and Mesh 2D in a small-scale wildfire monitoring area.

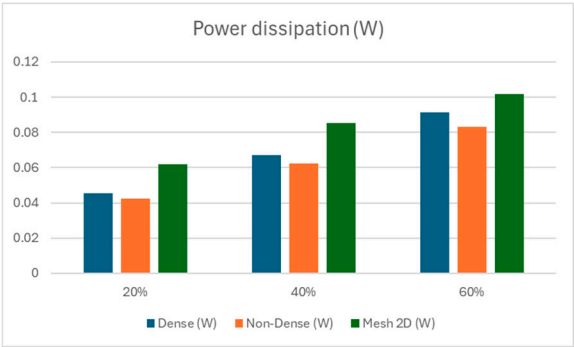


Figure 13. Power dissipation analysis in a 300 m coverage area.

Particularly, the non-dense topology shows higher energy efficiency at all fire diffusion rates (20%, 40%, 60%) compared to dense and Mesh 2D. This efficiency stems from its simplified single-tier architecture, which minimizes routing complexity, reduces hop counts, and avoids the overhead of dynamic inter-tier management needed in the dense topology. However, dense topologies excel in large-scale deployments through vertical rerouting and redundancy, their multi-layered design becomes counterproductive in confined areas, introducing unnecessary energy expenditure for maintaining tiered connections. In contrast, Mesh 2D topology leads to the highest energy consumption due to linear hop scaling and lack of adaptive routing, judging it inappropriate for dynamic wildfire environments. The non-dense topology’s lower energy demand also aligns with optimized duty cycling, where nodes prioritize sleep modes during low activity and employ efficient burst transmissions under higher fire rates. These findings emphasize the vital role of topology

adaptability: non-dense balances simplicity and functionality for small areas, whereas dense's strengths emerge in expansive, obstruction-rich terrains. The results validate the paper's emphasis on context-aware network design, promoting for topology choice based on deployment scale and environmental dynamics to improve energy sustainability in remote wildfire detection systems. Further investigation into advanced duty-cycling protocols and real-world validation could refine these models for broader applicability. These results align with theoretical predictions as given by Equation (15). In fact, the non-dense topology established higher energy efficiency in small-scale deployments due to reduced hop counts and simplified routing, while the dense topology's multi-tier overhead underperformed in confined areas, as expected. Mesh 2D's rigid grid structure confirmed its inefficiency, validating theoretical critiques of linear hop scaling and lack of adaptability in dynamic wildfire scenarios.

$$P_{total} = N[D(P_{tx} + P_{rx} + P_{idle}) + (1 - D)P_{sleep}] + C(h - 1)(P_{tx} + P_{rx}) \quad (15)$$

With:

- N: Number of nodes in the network.
- D: Duty cycle (fraction of time active), proportional to fire rate (e.g., D = 0.2 at 20% fire rate).
- P_{tx} , P_{rx} , P_{idle} , P_{sleep} : Power consumed in transmit, receive, idle, and sleep states.
- C: Number of data packets transmitted.
- h: Average hop count (depends on topology).

5. Conclusion

This paper describes an energy-efficient and scalable WSN architecture fitted for early wildfire detection in remote locations. By using a hybrid star/circular topology combined with adaptive routing protocols and round-robin dynamic arbitration, the proposed architecture exhibits sizable advances relatively to conventional Mesh 2D topologies. It realizes a 53–55% drop in node deployment, 41–81% lower latency, and 50–60% fewer routing hops. Simulation results shown over a 300 m radius confirm the advantage of the non-dense topology in energy consumption (0.0425–0.0832 W), while the dense configuration proves most effective in optimizing PLR, achieving up to an 80.4% reduction compared to Mesh 2D topologies.

Furthermore, the integration of artificial intelligence (multiclass logistic regression), allows high-precision fire risk prediction (99.97% in terms of accuracy) based on temperature and humidity sensor inputs. Combined with ZigBee and GSM technologies, the system guarantees robust communication in areas with limited or no internet coverage.

These results emphasize the system's practical advantages, involving cost-effective deployment, adaptability to diverse areas, and improved sensitivity to fire risks. This architecture provides a promising foundation for next-generation wildfire detection systems and has the potential to support open environmental examining initiatives globally.

Conflicts of Interest: The authors declare no conflict of interest.

References

1. Chowdary, V.; Gupta, M.K.; Singh, R. A Review on Forest Fire Detection Techniques: A Decadal Perspective. *Networks* **2018**, *4*(12).
2. Safford, H.D.; Paulson, A.K.; Steel, Z.L.; Young, D.J.; Wayman, R.B. The 2020 California Fire Season: A Year like No Other, a Return to the Past or a Harbinger of the Future. *Glob. Ecol. Biogeogr.* **2022**, *31*(10), 2005–2025.
3. Yu, L.; Wang, N.; Meng, X. Real-Time Forest Fire Detection with Wireless Sensor Networks. In Proceedings of the IEEE International Conference on Wireless Communications, Networking and Mobile Computing, Wuhan, China, September 2005; Volume 2, pp. 1214–1217.
4. Jin, L.; Yu, Y.; Zhou, J.; Bai, D.; Lin, H.; Zhou, H. SWVR: A Lightweight Deep Learning Algorithm for Forest Fire Detection and Recognition. *Forests* **2024**, *15*(1), 204.

5. Farej, Z.K.; Abdul-Hameed, A.M. Performance Comparison among (Star, Tree and Mesh) Topologies for Large Scale WSN based IEEE 802.15.4 Standard. *Int. J. Comput. Appl.* **2015**, *124*, 41–44.
6. Jaladi, A.R.; Khithani, K.; Pawar, P.; Malvi, K.; Sahoo, G. Environmental Monitoring Using Wireless Sensor Networks (WSN) Based on IoT. *Int. Res. J. Eng. Technol.* **2017**, *4*(1), 1371–1378.
7. Al-Karaki, J.N. Routing Techniques in Wireless Sensor Networks: A Survey. *IEEE Commun. Mag.* **2004**, *2*.
8. Atighi, I.; Zhou, Z. Safeguarding Forest Ecosystems: Harnessing IoT for Fire Detection. *Big Data Comput. Visions* **2023**, *3*(4), 146–153.
9. Choi, H.H.; Lee, K. Cooperative Wireless Power Transfer for Lifetime Maximization in Wireless Multihop Networks. *IEEE Trans. Veh. Technol.* **2021**, *70*(4), 3984–3989.
10. Kaur, P.; Kaur, K.; Singh, K.; Kim, S. Early Forest Fire Detection Using a Protocol for Energy-Efficient Clustering with Weighted-Based Optimization in Wireless Sensor Networks. *Appl. Sci.* **2023**, *13*(5), 3048.
11. Khan, F.; Xu, Z.; Sun, J.; Khan, F.M.; Ahmed, A.; Zhao, Y. Recent Advances in Sensors for Fire Detection. *Sensors* **2022**, *22*(9), 3310.
12. Ferdoush, S.; Li, X. Wireless Sensor Network System Design Using Raspberry Pi and Arduino for Environmental Monitoring Applications. *Procedia Comput. Sci.* **2014**, *34*, 103–110.
13. Vijayan, S.G.; Rahman, N.A.A.; Harun, K.S. A Conceptual Framework of Zigbee Wireless Sensor Networks for Safety, Reliability and Security Improvement. In Proceedings of the AIP Conference; AIP Publishing: January 2024; AIP Conf. Proc. 2024, 2802(1).
14. Alvares, B.; Perez, E.; Trigueros, J.; Ho, J.; Ly, E.; Le, H.T. Development of a Solar-Powered Wildfire Detector System for Remote Locations with XBee and GSM Capabilities. *WSEAS Trans. Comput.* **2021**, *20*, 189–198.
15. Dasari, P.; Reddy, G.K.J.; Gudipalli, A. Forest Fire Detection Using Wireless Sensor Networks. *Int. J. Smart Sens. Intell. Syst.* **2020**, *13*(1), 1–8.
16. Ganesan, R.; Pulloor, K.; Devika, R.; Kumar, N.R.; Devi, S.S. Forest Fire Monitoring System Based on GPRS and Zigbee Wireless Sensor Networks. *Forest* **2015**, *4*(6).
17. Somov, A. Wildfire Safety with Wireless Sensor Networks. EAI Endorsed Trans. *Ambient Syst.* **2011**, *1*(1).
18. Gomathi, C.; Vennila, K.; Sathyananth, M.; Shriarthi, B.; Selvarasu, S. Forest Fire Detection Using Wireless Sensor Network. *Int. J. Eng. Res. Technol. (IJERT)* **2015**, *3*(12), 1–4.
19. Sabit, H.; Al-Anbuky, A.; GholamHosseini, H. Wireless Sensor Network-Based Wildfire Hazard Prediction System Modeling. *Procedia Comput. Sci.* **2011**, *5*, 106–114.
20. Bahrepour, M.; Meratnia, N.; Havinga, P.J. Use of AI Techniques for Residential Fire Detection in Wireless Sensor Networks. In Proceedings of the 5th IFIP Conference on Artificial Intelligence Applications & Innovations (AIAI 2009); CEUR: July 2009; pp. 311–321.
21. Ko, A.; Lee, N.M.Y.; Sham, R.P.S.; So, C.M.; Kwok, S.C.F. Intelligent Wireless Sensor Network for Wildfire Detection. *WIT Trans. Ecol. Environ.* **2012**, *158*, 137–148.
22. Pradeep, S.; Sharma, Y.K.; Verma, C.; Constantin, N.B.; Illés, Z.; Raboaca, M.S.; Mihaltan, T.C. Utilizing WSN and Artificial Intelligence to Detect Fires. In Proceedings of the 2022 11th IEEE International Conference on System Modeling & Advancement in Research Trends (SMART); IEEE: December 2022; pp. 424–428.
23. Varela, N.; Ospino, A.; Zelaya, N.A.L. Wireless Sensor Network for Forest Fire Detection. *Procedia Comput. Sci.* **2020**, *175*, 435–440.
24. Maher, W.A.; Baraa, A.; Abu, Z.; Nidal, H.N.; Ruba, R.A.; Aya, Haider, A.; Samy, S.A. Predicting Fire Alarms in Smoke Detection Using Neural Networks. *Int. J. Acad. Inf. Syst. Res. (IJASIR)* **2023**, *7*(10), 26–33.
25. Jaspreet, K.B.; Shreyas, A.R.; Siddhant, B.; Shane, L.; Eugene, Z.; Ravi, R.; Harrison, K.; Chris, S.; Chris, A.J.; Block, I.P.; Daniel, C.; Ilkay, A.; Garrison, W.C.; Mai, H.N. Multimodal Wildland Fire Smoke Detection. *Remote Sens.* **2023**, *15*(11), 2790.
26. Yang, H.; Zhou, H.; Liu, Z.; Deng, X. Energy Optimization of Wireless Sensor Embedded Cloud Computing Data Monitoring System in 6G Environment. *Sensors* **2023**, *23*(2), 1013. <https://doi.org/10.3390/s23021013>.
27. Benzekri, W.; El Moussati, A.; Moussaoui, O.; Berrajaa, M. Early Forest Fire Detection System Using Wireless Sensor Network and Deep Learning. *Int. J. Adv. Comput. Sci. Appl.* **2020**, *11*(5).

28. Mahdianpari, M.; Ahmadi, S.A.; Marjani, M. FirePred: A Hybrid Multi-Temporal Convolutional Neural Network Model for Wildfire Spread Prediction. *Ecol. Inform.* **2023**, *78*, 102282.
29. Avazov, K.; Hyun, A.E.; Sami S, A.A.; Khaitov, A.; Abdusalomov, A.B.; Cho, Y.I. Forest Fire Detection and Notification Method Based on AI and IoT Approaches. *Future Internet* **2023**, *15*(2), 61.
30. Mulligan, R.; Ammari, H.M. Coverage in Wireless Sensor Networks: A Survey. *Netw. Protoc. Algorithms* **2010**, *2*(2), 1–22. <https://doi.org/10.5296/npa.v2i2.276>.
31. Abbasi, M.; Abd Latiff, M.S.B.; Chizari, H. An Overview of Distributed Energy-Efficient Topology Control for Wireless Ad Hoc Networks. *Math. Probl. Eng.* **2013**, *2013*, 126269.
32. Jiang, R. A Review of Network Topology. In *Proceedings of the 4th International Conference on Computer, Mechatronics, Control and Electronic Engineering*; Atlantis Press: Paris, France, 2015; pp. 1167–1170.
33. Chéour, R.; Jmal, M.W.; Khriji, S.; El Houssaini, D.; Trigona, C.; Abid, M.; Kanoun, O. Towards Hybrid Energy-Efficient Power Management in Wireless Sensor Networks. *Sensors* **2021**, *22*(1), 301.
34. Kurose, J.F.; Ross, K.W. *Computer Networking: A Top-Down Approach*, 8th ed.; Pearson: Boston, MA, USA, 2021.
35. Riley, G.F.; Henderson, T.R. The ns-3 Network Simulator. In *Modeling and Tools for Network Simulation*; 2010.
36. Vu, K.Q.; Ban, N.T.; Nam, V.H.; Han, N.D. Survey of Recent Routing Metrics and Protocols for Mobile Ad-Hoc Networks. *J. Commun.* **2019**, *14*(2), 110–120.
37. Zeeshan, M.; Ali, A.; Naveed, A.; Liu, A.X.; Wang, A.; Qureshi, H.K. Modeling Packet Loss Probability and Busy Time in Multi-Hop Wireless Networks. *EURASIP J. Wirel. Commun. Netw.* **2016**, 168.
38. Daintree Networks. Getting Started with ZigBee and IEEE 802.15.4; Daintree Networks Inc.: 2008. Available online: <https://www.science.smith.edu/~jcardell/Courses/EGR328/Readings/Zigbee%20GettingStarted.pdf>
39. Yang, Y.; Wu, R.; Zhang, L.; Zhou, D. An Asynchronous Adaptive Priority Round-Robin Arbiter Based on Four-Phase Dual-Rail Protocol. *Chin. J. Electron.* **2015**, *24*(1), 1–7.
40. Oveis-Gharan, M.; Khan, G.N. Index-Based Round-Robin Arbiter for NoC Routers. In *Proceedings of the 2015 IEEE Computer Society Annual Symposium on VLSI*; IEEE: 2015; pp. 62–67.
41. Monemi, A.; Ooi, C.Y.; Palesi, M.; Marsono, M.N. Ping-Lock Round Robin Arbiter. *Microelectron. J.* **2017**, *63*, 81–93.
42. Parvathi, S.; Umamaheswari, S. Load Based Dynamic Priority Arbiter for NoC Architecture. *J. Sci. Ind. Res.* **2022**, *81*(05), 495–504.
43. Naqvi, S.R.; Akram, T.; Haider, S.A.; Kamran, M. Artificial Neural Networks Based Dynamic Priority Arbitration for Asynchronous Flow Control. *Neural Comput. Appl.* **2018**, *29*, 627–637.
44. Dobkin, R.R.; Ginosar, R.; Kolodny, A. QNoC Asynchronous Router. *Integration* **2009**, *42*(2), 103–115.
45. Younis, M.; Bushra, S. Efficient Distributed Medium Access Arbitration for Multi-Channel Wireless Sensor Networks. In *Proceedings of the 2007 IEEE International Conference on Communications*; IEEE: June 2007; pp. 3666–3671.
46. Khalaf, O.I.; Romero, C.A.T.; Hassan, S.; Iqbal, M.T. Mitigating Hotspot Issues in Heterogeneous Wireless Sensor Networks. *J. Sens.* **2022**, *2022*(1), 7909472.
47. Hussain, K.; Xia, Y.; Onaizah, A.N. Starvation Mitigation and Priority Aware of CSMA/CA in WSN with Implementing Markov Chain Model. *Optik* **2022**, *271*, 170186.
48. Yang, P.T.; Chen, C.J. Conflict Detection in Interval-Based Sequences from Wireless Sensor Networks. In *Proceedings of the 2017 International Conference on Information Technology*; 2017; pp. 263–267.
49. Ying, B.; Liu, W.; Liu, Y.; Yang, H.; Wang, H. Energy-Efficient Node-Level Compression Arbitration for Wireless Sensor Networks. In *Proceedings of the 2009 11th IEEE International Conference on Advanced Communication Technology*; IEEE: February 2009; Volume 1, pp. 564–568.
50. Wang, L.; Zhao, Q.; Wen, Z.; Qu, J. RAFFIA: Short-Term Forest Fire Danger Rating Prediction via Multiclass Logistic Regression. *Sustainability* **2018**, *10*(12).
51. Alahmari, B. Predicting Weather in Saudi Arabia by Using Machine Learning. Medium 2022. Available online: https://medium.com/@Bashayer_Alahmari/predicting-weather-in-saudi-arabia-by-using-machine-learning-30317fe1dcf5
52. Bounceur, A.; Bezoui, M.; Euler, R.; Lalem, F. CupCarbon: A Multi-Agent and Discrete Event Wireless Sensor Network Simulator for the Internet of Things and Smart Cities. *Future Internet* **2017**, *9*(4), 77.

53. Kumar, A.; Sharma, R. Simulation of Wireless Sensor Networks for Environmental Monitoring Using Proteus. In Proceedings of the 5th International Conference on Advances in Robotics, Automation, and Data Science (ICARAD); 2021; pp. 1–6.
54. Sonawane, R.N.; Ghule, A.S.; Bowlekar, A.P.; Zakane, A.H. Design and Development of Temperature and Humidity Monitoring System. *Agric. Sci. Dig.* **2019**, *39*(2), 114–118.
55. Chamorro Atalaya, O.; Arce Santillan, D. Fire Alert System through Text Messages, with Arduino Mega Technology and GSM SIM 900 Module. *Indones. J. Electr. Eng. Comput. Sci.* **2020**, *18*(3), 1215–1221.
56. Camilo, T.; Rodrigues, A.; Silva, J.S.; Boavida, F. Redes de Sensores Sem Fios, Considerações sobre a Sua Instalação em Ambiente Real. In Wireless Sensor Networks – Some Considerations on Deployment in Real Environments, CSMU2006; Guimarães, Portugal, June 2006.
57. Heinzelman, W.B.; Chandrakasan, A.P.; Balakrishnan, H. Energy-Efficient Communication Protocol for Wireless Microsensor Networks (LEACH). In Proceedings of the 33rd Annual Hawaii International Conference on System Sciences; IEEE: January 2000.

Disclaimer/Publisher’s Note: The statements, opinions and data contained in all publications are solely those of the individual author(s) and contributor(s) and not of MDPI and/or the editor(s). MDPI and/or the editor(s) disclaim responsibility for any injury to people or property resulting from any ideas, methods, instructions or products referred to in the content.